

New insights in the origin and evolution of the old, metal-rich open cluster NGC 6791

Luis A. Martinez-Medina^{1*}, Mark Gieles², Barbara Pichardo¹, Antonio Peimbert¹

¹ Instituto de Astronomía, Universidad Nacional Autónoma de México, A.P. 70–264, 04510, México, CDMX, México

² Department of Physics, University of Surrey, Guildford, GU2 7XH, UK

30 October 2017

ABSTRACT

NGC 6791 is one of the most studied open clusters, it is massive ($\sim 5000 M_{\odot}$), located at the solar circle, old (~ 8 Gyr) and yet the most metal-rich cluster ($[Fe/H] \simeq 0.4$) known in the Milky Way. By performing an orbital analysis within a Galactic model including spiral arms and a bar, we found that it is plausible that NGC 6791 formed in the inner thin disc or in the bulge, and later displaced by radial migration to its current orbit. We apply different tools to simulate NGC 6791, including direct N -body summation in time-varying potentials, to test its survivability when going through different Galactic environments. In order to survive the 8 Gyr journey moving on a migrating orbit, NGC 6791 must have been more massive, $M_0 \geq 5 \times 10^4 M_{\odot}$, when formed. We find independent confirmation of this initial mass in the stellar mass function, which is observed to be flat; this can only be explained if the average tidal field strength experienced by the cluster is stronger than what it is at its current orbit. Therefore, the birth place and journeys of NGC 6791 are imprinted in its chemical composition, in its mass loss, and in its flat stellar mass function, supporting its origin in the inner thin disc or in the bulge.

Key words: Galaxy: disc — Galaxy: kinematics and dynamics — open clusters and associations: general — open clusters and associations: individual: NGC 6791 — Galaxy: structure

1 INTRODUCTION

Open clusters form in the thin molecular gas disc of the Galaxy (de la Fuente Marcos & de la Fuente Marcos 2008), within a galactocentric distance of ~ 10 kpc and closer than 180 pc away from the disc plane (Dias et al. 2002; Gozha et al. 2012). No more than 10% survive their emergence from molecular clouds as bound systems (Lada & Lada 2003). They range in age between a few million years and approximately 10 Gyr, and are currently located between 5 and 20 kpc from the Galactic centre (Freeman 1970; Nagata et al. 1993; Krabbe et al. 1995; Figer et al. 2002; van der Kruit 2002; Paumard et al. 2006; Davies et al. 2012; Moreno et al. 2014; Ramírez Alegría et al. 2014). From the estimated 10^5 open clusters existing today (Portegies Zwart et al. 2010; Piskunov et al. 2006), we only know a few thousand due to large amounts of reddening and crowding, especially towards the Galactic centre (van der Kruit 2002; Freeman 1970). Only a few clusters are near enough to be well studied and portrayed.

From all open clusters in the solar neighbourhood, NGC 6791 is probably the most intriguing, because of its remarkable orbital and physical characteristics. With a distance of 4 kpc from the Sun, this cluster is located close to the solar circle at 8 kpc from the Galactic centre and 0.8 kpc above the plane. It is an 8 Gyr old system, which makes it the oldest open cluster known (Brogaard et al. 2012; García-Berro et al. 2010; Grundahl et al. 2008; King et al. 2005; Kinman 1965), and the most metallic with $[Fe/H] \sim +0.40$ (Carraro et al. 2006; Gratton et al. 2006; Origlia et al. 2006). NGC 6791 is also one of the most massive open clusters with $M \sim 5000 M_{\odot}$ (Platais et al. 2011); this means that the cluster either traveled through the Galaxy on a relatively quiet orbit or it was born with a much larger initial mass. In particular, due to its current mass and height above the Galactic plane, NGC 6791 seems to have been formed as a cluster intermediate between an open and a globular cluster (Kinman 1965).

The initial mass parameter is difficult to determine since it depends not only on the environment where it was born but also depends strongly on the characteristics of the orbit it followed since its formation (e.g., encounters with the spi-

* Contact e-mail: lamartinez@astro.unam.mx

ral arms (Gieles, Athanassoula, & Portegies Zwart 2007), interactions with the bulge and disc tidal fields), as well as on its intrinsic stellar evolution and two-body relaxation. Regarding the calculation of NGC 6791 initial mass, work has been done based on observations combined with theoretical work; the first to estimate the total mass of the cluster was Kinman (1965), who found a mass of $\sim 3700 M_{\odot}$, considering only stars with $m_V < 20$. Later on Kaluzny & Udalski (1992), confirm the observations but suggest that a significant fraction of the mass lies in fainter stars. More recently, Dalessandro et al. (2015) derive an initial mass for the cluster in the range $M = (1.5-4) \times 10^5 M_{\odot}$, using an expression for the mass evolution of clusters evolving in the Milky Way disc from Lamers et al. (2005).

Several numerical efforts have been done in the past few years to obtain the orbit of this cluster, which in turn could provide information on its origin within the Galaxy. Some examples are: Bedin et al. (2006), who obtain an orbit of approximately 10 kpc of average radius and an eccentricity of 0.5; Wu et al. (2009), who obtain a similar radius but with an eccentricity of 0.3 (these two studies were simulated in simple axisymmetric potentials); or Carraro et al. (2006), who find a distance beyond 20 kpc with an eccentricity of 0.59.

The most recent and complete calculation of NGC 6791 orbit was performed by Jilková et al. (2012). In that work the authors present a numerical study of the orbit that includes the combined effect of the bar and spiral arms in a Galactic disc and halo potential. However, the non-axisymmetric part of the model employed by the authors for the spiral arms (Cox & Gómez 2002), for instance, does not represent any known mass distribution, i.e., this model for the spiral arms is a local approximation (as it is based on the addition of sine and cosine functions), this means it is not based on a density distribution but it is instead a mathematical ad hoc approximation; this type of spiral arm models are intrinsically smooth and symmetrical functions that might underestimate the effect of spiral arms on the general gas and stellar dynamics.

Alternatively, the peculiar orbit and high [Fe/H] of NGC 6791 may point at an extragalactic origin: in that scenario the cluster, as it is currently, could be a remnant of an initially more massive cluster that experienced severe disruption by the MW tides, however Linden et al. (2017); Cunha et al. (2015); Carraro et al. (2006), find a small chemical abundance spread, unlike the one normally seen in the local group dwarf galaxies (Mateo 1998).

Could an open cluster with such a peculiar combination of parameters have formed within the Milky Way? (i.e., age, high metallicity, mass, altitude over the Galactic plane and current galactocentric distance). Since stars with similar metallicity to the ones within this cluster have been found in the Galactic bulge (Bensby et al. 2013), Jilková et al. (2012) suggested the possibility that the cluster originated in the bulge, where star formation was rapid and efficient enough to generate it, however they concluded this scenario had a very low probability. Of course, determining the Galactic orbit and survival of the cluster NGC 6791 poses a challenge for several reasons. Firstly, to restrict the orbit one depends on the quality of kinematic data. Secondly, a realistic model of the Milky Way is required, since the orbital behaviour depends on the details of the spiral arms and bar

representation. Additionally, a good modeling of the internal dynamics due to stellar evolution, two-body relaxation, and the interaction with the Galactic tides is key when studying the cluster's disruption along its path through the Galaxy.

In this work, we explore possible locations for the formation of NGC 6791, improving previous determinations by including, among other things, a more detailed model of the MW Galaxy, as well as a more rigorous criteria in the selection of the orbits. Unlike other determinations (e.g. Jilková et al. 2012), we show there is a good probability that NGC 6791 was born in the inner thin disc or in the Galactic bulge region, where an open cluster of such mass and metallicity is likely to form; we explain in this paper the reasons for the different results between these authors and our results. We also present two studies on the survivability of NGC 6791, one based on a self-consistent field technique and other based on direct N -body models.

This paper is organized as follows. In Section 2, the Galactic model, the clusters model, the initial conditions, and the methodology employed are presented. Section 3 presents the orbital analysis and radial migration scenario. Section 4 shows the studies of likelihood of survival for NGC 6791 through different Galactic environments. Section 5 shows our N -body computations of NGC 6791. A brief discussion is presented in Section 7. Finally, in Section 8, we present our conclusions.

2 GALACTIC MASS MODEL

For the Galactic model we employ a three dimensional potential with disc, halo, and rotating spiral-arm and bar components, that fits the structural and dynamical parameters to the best we know of the recent knowledge of the Galaxy. We present a summary of the model; a full description of this potential and its updated parameters appears in a score of papers (Martinez-Medina et al. 2015, 2017; Pichardo et al. 2003, 2004, 2012; Moreno et al. 2015). We chose to use this Galactic model over the use of the more sophisticated N -body simulations because they are not applicable to reach the objectives of this work: firstly, because our model is completely adjustable to better simulate what we know of the MW (contrary to N -body simulations). Secondly, because it is significantly faster and therefore more suitable for statistical studies like the ones presented in this paper. Finally, this type of models allows us to study in detail orbital behaviour without the resolution problems of N -body simulations.

The model is constituted by an axisymmetric background potential and a non-axisymmetric one. The axisymmetric potential consists of a Miyamoto-Nagai disc (Miyamoto & Nagai 1975) with a vertical height of 250 pc, a Miyamoto-Nagai spherical bulge, and dark matter spherical halo (based on the potential of Allen & Santillán 1991). The non-axisymmetric part includes a three dimensional spiral arms potential and a bar. The Galactic potential is scaled to the Sun's galactocentric distance, 8.5 kpc, and the local rotation velocity, 220 km s^{-1} .

Regarding the non-axisymmetric part of the Galaxy, observations in infrared bands such as those of the COBE/DIRBE K-band and the infrared Spitzer/GLIMPSE survey, seem to show that two of the observed arms are dominant (Drimmel & Spergel 2001; Churchwell et al.

2009). Additionally, based on theoretical work that has shown that two (or more) additional gaseous arms can form (without increasing the stellar surface density) as a response to a two-armed dominant pattern (Martos et al. 2004; Pérez-Villegas et al. 2015), in this work we will adopt a two-armed structure for the spiral arms, simulating the main Galactic spiral arms based on the Spitzer/GLIMPSE database (Benjamin et al. 2005; Churchwell et al. 2009). For the spiral arms potential, we employ a model formed by a bisymmetric three-dimensional density distribution built of individual inhomogeneous oblate spheroids (PERLAS model Pichardo et al. 2003) that are placed as bricks in a building within a logarithmic spiral locus. The density falls exponentially along the arms. The total mass of the spiral arms taken in these experiments is $4.28 \times 10^9 M_{\odot}$, that corresponds to a mass ratio of $M_{\text{arms}}/M_{\text{disc}} = 0.05$. Finally, for the angular velocity, we employ a value of $\Omega_S = 20 - 28 \text{ km s}^{-1} \text{ kpc}^{-1}$, motivated by different observational and theoretical methods (Martinez-Medina et al. 2017; Gerhard 2011).

For the bar potential we selected the triaxial inhomogeneous ellipsoid of Pichardo et al. (2004); this is a superposition of homogeneous ellipsoids made to reach a smooth density fall that approximates the density fall fitted by Freudenreich (1998) from the COBE/DIRBE observations of the Galactic centre. The total mass of the bar is $1.4 \times 10^{10} M_{\odot}$, within the observational limits (e.g., Kent 1992; Zhao 1994; Dwek et al. 1995; Blum 1995; Stanek et al. 1997; Weiner & Sellwood 1999; Antoja et al. 2014). Finally, the angular speed is observationally set within the range: $\Omega = 45 - 55 \text{ km s}^{-1} \text{ kpc}^{-1}$ (Antoja et al. 2009; Gerhard 2011, and references therein).

For a detailed list of the parameters adopted here to simulate the Galaxy, see in particular Section 2 of Martinez-Medina et al. (2017). Brief descriptions and remainders of the parameters employed on each simulation of this study are presented across the paper.

3 ORBITAL ANALYSIS / RADIAL MIGRATION SCENARIO

As suggested by its high [Fe/H], the location of formation of NGC 6791, should be far away from its current galactocentric position: it may have formed in the inner thin disc or in the bulge. However, placing its birth near the Galactic centre could be a major challenge: it requires a dynamical mechanism to move the cluster from the inner Galaxy to its current position at the solar circle; in addition, we need to assess the probability for this mechanism to happen.

The orbit of the cluster can be moved to larger radii by increasing its angular momentum. It is known that radial migration occurs when a star exchanges angular momentum with the non-axisymmetric structures in the disc, changing permanently the guiding radius of the orbit. Radial migration is expected to be more efficient when it is driven by a transient spiral pattern (Sellwood & Binney 2002), however, simulations show that it can also be triggered by the combined presence of a bar and spiral arms, which can displace orbits radially without a significant increase in its eccentricity (Martinez-Medina et al. 2016; Monari et al. 2016; Martinez-Medina et al. 2017).

In this section we explore whether radial migration oc-

Table 1. Galactic mass models constructed for the orbital analysis.

Model	Pattern speeds ($\text{km s}^{-1} \text{ kpc}^{-1}$)	
	Bar	Spiral Arms
A	45	20
B	45	28
C	55	20
D	55	28

curs in our MW mass model, as well as which combinations, of dynamical parameters for the bar and spirals, are more efficient in bringing orbits from the inner disc to the solar circle.

In order to perform this orbital analysis, we first construct four MW mass models, as described in the previous section; these models differ in the pattern speeds of the bar and spirals. Table 1 indicates the combination of pattern speeds used for each MW mass model. We then populate each model with a particle disc distribution composed of 500,000 test particles, and finally integrate their orbits for 8.5 Gyr. From these orbits, we pick those that at the end of the simulation have similar positions, proper motions, and radial velocities (within 2σ) to the current ones for NGC 6791.

The coordinates assumed for NGC 6791 are computed as follows: from the current heliocentric equatorial coordinates, proper motion, parallax, and radial velocity of NGC 6791 (see Table 2), and the formula by Johnson & Soderblom (1987, updated to the International Celestial Reference System), we obtain the kinematics in coordinates centred on the Sun; the transformation returns, in a right-handed cylindrical coordinate system, the radial, rotational, and vertical components of the velocity (U, V, W), that are positive in the direction of the GC, Galactic rotation, and north Galactic pole, respectively. Then, by placing the Sun at $(X, Y, Z)_{\odot} = (8.5, 0.0, 0.025) \text{ kpc}$, adopting the Sun's velocity with respect to the LSR $(U, V, W)_{\odot} = (11.1, 12.24, 7.25) \text{ km s}^{-1}$ (Schönrich et al. 2010), and a $V_{\text{LSR}} = 220 \text{ km s}^{-1}$, we compute the translation from a coordinate frame centred on the Sun to a cylindrical coordinate frame centred on the Galaxy (Table 2).

We note that Jílková et al. (2012) use different velocities; unfortunately, they omitted to rotate U and V by $\sim 28^{\circ}$ to obtain the correct Cartesian velocities (since the position vector of NGC 6791 is not aligned with the X -axis), before computing their orbits. This missing step in the calculations by Jílková et al. leads to a misrepresentation of the orbit of NGC 6791, that in turn leads to underestimate the efficiency of the migration mechanism (in Private communication with Jílková et al., after fixing the omitted velocity rotation, their re-calculated efficiency of displacing the orbit of NGC 6791 to its current position increases by an order of magnitude).

In addition, although these authors start from very precise proper motion and radial velocity, these values are only used to compute an average peri-galacticon and apogalacticon for the present orbit of NGC 6791, which in turn are the ones used for their orbital analysis; in this manner, the precise information of the observed kinematics of

Table 2. Adopted observational data for NGC 6791

<i>Equatorial coordinates, radial velocity, PM, distance to the Sun.</i>		
	<i>Value</i>	<i>Reference</i>
α	290.22083°	(1)
δ	37.77167°	(1)
v_r	$-47.1 \pm 0.7 \text{ km s}^{-1}$	(2)
$\mu_\alpha \cos \delta$	$-0.57 \pm 0.13 \text{ mas yr}^{-1}$	(2)
μ_δ	$-2.45 \pm 0.12 \text{ mas yr}^{-1}$	(2)
d_\odot	$4.01 \pm 0.14 \text{ kpc}$	(3)
<i>Galactocentric coordinates</i>		
	<i>Value</i>	
R_{GC}	$8.05 \pm 0.36 \text{ kpc}$	
Z	$0.78 \pm 0.0315 \text{ kpc}$	
U	$39.8 \pm 3.9 \text{ km s}^{-1}$	
V	$174.74 \pm 3.3 \text{ km s}^{-1}$	
W	$-12.13 \pm 3.0 \text{ km s}^{-1}$	

(1) WEBDA; (2) [Bedin et al. \(2006\)](#); (3) [Brogaard et al. \(2011\)](#)

the cluster is diluted, making it impossible to identify any possible chaotic behaviour in the orbit of the cluster.

3.1 Migrating orbits

Once we have the current galactocentric position and velocities for NGC 6791, we analyse our integrated orbits and pick the ones with all their parameters similar to those of Table 2. First we assume a cluster age of $8.0 \pm 0.5 \text{ Gyr}$, so we look for orbits in the $[7.5, 8.5] \text{ Gyr}$ age interval. From those orbits we select the ones that meet the criteria of having $(R, Z) \in (R \pm 2\sigma_R, Z \pm 2\sigma_Z)_{\text{NGC 6791}}$ and $(U, V, W) \in (U \pm 2\sigma_U, V \pm 2\sigma_V, W \pm 2\sigma_W)_{\text{NGC 6791}}$, where the observational uncertainty is taken as the dispersion σ .

The complete procedure for this orbital selection is as follows: for the entire set of orbits first we constrain on R and Z ; then, for those orbits the rotation velocity is computed $V = (Y/R)V_X - (X/R)V_Y$ and we select the ones with $V \approx V_{\text{NGC6791}}$; similarly, we further constrain on radial velocity $U = -(X/R)V_X - (Y/R)V_Y$ with the condition $U \approx U_{\text{NGC6791}}$. Finally, the last constraint for the remaining orbits is to have $W = V_Z \approx W_{\text{NGC6791}}$.

The result of this analysis, performed in our four Galactic models is presented in Figure 1. The figure shows the initial galactocentric radius (left column) and initial height above the Galactic plane (right column) for the orbits that meet the selection criteria.

The final point of each of these orbits has very similar position and velocity to the current one of NGC 6791; Figure 1 shows their birth positions. The first thing to notice is that, although all selected orbits end at 8 kpc from the Galactic centre, most of them come from the inner disc; this is a common trend in our four Galactic models, and all of them show that an orbit like that of NGC 6791 (Table 2) is more likely to have come from smaller radii, with the highest probabilities between $5 < R_0/\text{kpc} < 8$.

Model B is the one with the widest initial radii distribution, which implies radial displacements induced over a greater region of the disc. Also, for this model the mean value of the initial radius is the lowest, $\langle R_0 \rangle = 6.37 \text{ kpc}$, i.e.,

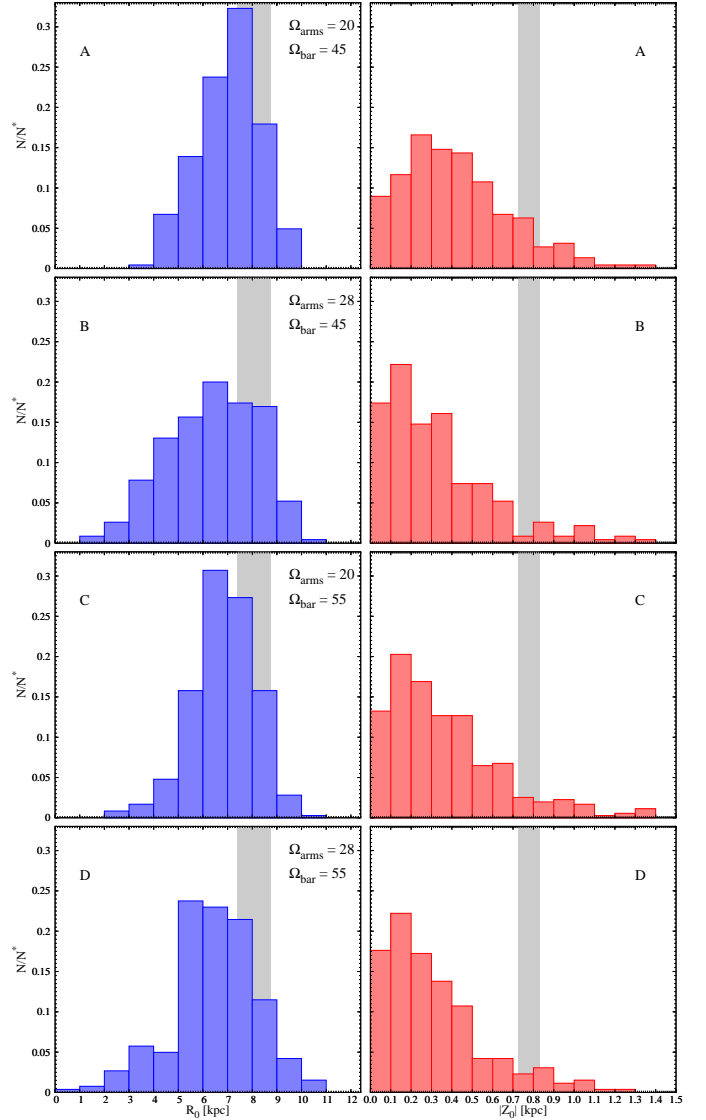


Figure 1. Distribution of initial galactocentric radii, R_0 , and initial vertical separation from the plane, $|z_0|$, for orbits that meet our criteria (i.e. with kinematics similar to those of NGC 6791, see text). The grey bands show the final R and z values of those orbits. N is the number of orbits at a given initial radius and N^* is the total number of selected orbits. The adopted values for Ω_{arms} and Ω_{bar} are indicated in units of $\text{km s}^{-1} \text{ kpc}^{-1}$.

this combination of pattern speeds for bar and spiral arms is more efficient in bringing orbits from the inner disc to the solar circle.

Additionally, because we are invoking the mechanism of radial migration to explain the high metallicity of NGC 6791, at odds with its age and current position, we look for orbits formed within the specific radial range $3 < R_0/\text{kpc} < 5 \text{ kpc}$. Figure 1 shows that such orbits exist, and although the probability of finding them is greater in model B, these orbits exist in all four Galactic models, which means that they are not restricted to a particular combination of pattern speeds.

A final requirement for the orbit of NGC 6791 is to start near the Galactic plane ($Z \sim 0$), because that is where the

cold molecular gas is from which the cluster formed. Figure 1 (left column) shows that most of the displaced orbits start their evolution within the thin disc, with a significant probability of being formed very close to the Galactic plane. Again, model B is the most efficient in bringing orbits from the Galactic plane to altitudes of ~ 800 pc (to match the current vertical position of NGC 6791). Because both the lifting of the orbits as well as the exchange of angular momentum are more efficient for orbits interacting more time with the non-axisymmetric structures of the disc, it is expected for model B, the one inducing larger radial displacements, to be the one more efficient in bringing orbits from the thin disc to high altitudes.

We find 240 orbits out of the 257,352 that originate between 3 and 5 kpc in our model, that match (within 2σ) the current orbital parameters of NGC 6791. If we were interested only in matching the position, the number of orbits increases to 3239. This scenario explains naturally its high metallicity, in spite of its old age and large Galactocentric radius.

3.2 Likelihood of observing an anomalous open cluster, like NGC 6791, in the solar neighbourhood

To understand the likelihood of the existence of a cluster like NGC 6791 in our Galaxy, one should not compare the fraction of orbits that match NGC 6791, but rather look for the fraction of orbits that would produce an anomalous object similar to NGC 6791, and to figure out, for each of these orbits, which fraction of the time they would appear to be anomalous.

To do this, we first need to determine the criteria that define an orbit as anomalous (in the NGC 6791 sense). The orbits we are interested in started between 7.5 and 8.5 Gyr ago, near the galactic plane, with a galactocentric radius between 3 and 5 kpc. We consider them to produce an “interesting orbit” if, at the present time, they are far away from the Galactic plane, have migrated outwards at least 2 kpc (i.e. have an anomalously high metallicity), and are observable from Earth; quantitatively we require these orbits to be at least 500 pc away from the galactic plane, with a galactocentric radius of at least 7 kpc, but at most 8 kpc away from the Sun.

We explored 257,352 orbits, and for each orbit, we took a hundred snapshots (to represent the range of valid ages for the cluster); out of these 25,735,200 possible events, we found 61,208 that met our criteria; i.e one out of each 420 events would produce such an object. This means that, if approximately 420 moderately massive clusters were formed between 7.5 and 8.5 Gyr ago, in the Galactic plane with a galactocentric radius between 3 and 5 kpc, we would expect to observe today an object like NGC 6791 (we will see in Section 5.1 that we need 420 clusters with an initial mass of at least 50,000 solar masses).

As a result of the orbital analysis in this section, we have shown that it is plausible that NGC 6791 formed in the inner thin disc or even in the bulge region.

4 SURVIVABILITY OF NGC 6791 THROUGH DIFFERENT GALACTIC ENVIRONMENTS

In the previous section we have shown that it is possible that NGC 6791 was born in the inner thin disc or bulge and suffered an outward radial migration that brought the cluster to its current position. An important question for this evolution scenario remains: is the cluster able to survive this? Not only do we need a dynamical mechanism that displaces the orbit, but also the cluster must manage to survive its journey from the inner disc to the solar circle.

In Section 3, we found several possible orbits for NGC 6791; in this section we study whether the cluster can survive the ~ 8 Gyr evolution moving on these orbits, and under which conditions it can be done.

4.1 Modeling stellar clusters with a self-consistent field technique

The disruption time depends on the strength of the Galactic tides (directly related to the type of orbit), initial mass, and size of the cluster. Modeling NGC 6791, and analysing its disruption time, for several combinations of these three factors requires hundreds of simulations. Due to the computation time, this is not viable to do with a direct N -body code. Instead, for this part of the work, we use the technique described in [Martinez-Medina et al. \(2017\)](#) to model NGC 6791. The method assumes that the cluster is spherically symmetric such that the gravitational potential can be approximated with that of a [Plummer \(1911\)](#) model, which corresponds to the zeroth order member in a basis expansion of the gravitational potential ([Clutton-Brock 1972, 1973; Hernquist & Ostriker 1992](#)). In order to capture mass loss, the criteria to decide the membership of a given star to the cluster is that the star’s velocity, v , must be less than the local escape velocity, v_{esc} . Those stars with $v > v_{\text{esc}}$ are removed from the cluster, which will cause the cluster to lose mass. This definition of v_{esc} does not include the contribution of the tides to the (Jacobi) energy of the stars, mainly because this is ill-defined when the tides are time-dependent. [Renaud, Gieles, & Boily \(2011\)](#) used N -body simulations of clusters on circular orbits to show that this simple escape criterion results in a bound mass evolution that is similar to models in which the tides are included in the definition of v_{esc} . In addition, the radial scale of the Plummer potential evolves with time by computing, at each time step, the half-mass radius, r_h , of the distribution, which for the Plummer profile is related to the radial scale-length, a , as $r_h \approx 1.3a$. In this way, the potential of the cluster, although assumed to be represented by a Plummer model, is evolving with time, with the ability of mimicking expansions and contractions, as well as the mass loss of the system.

In this method, stars in the cluster do not interact with one another directly; instead, the contribution of all of them create the global potential in which the stars orbit. This is an efficient technique that allows us to approach the self-gravity of the cluster with minimal computational overhead. By avoiding two-body relaxation, this technique isolates the effect of tidal interaction of the cluster with the Galaxy.

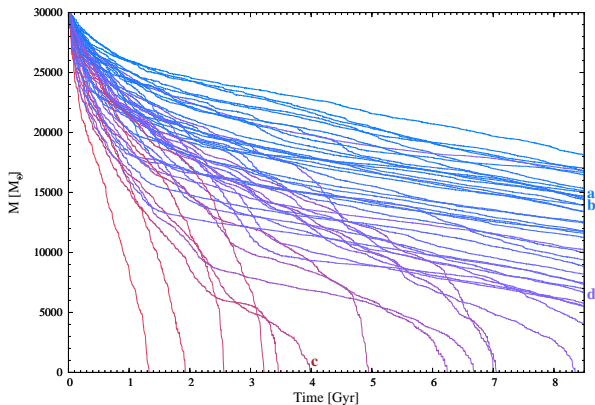


Figure 2. Mass evolution for the stellar cluster evolved along the orbits integrated with the Galactic model B, and that meet the criteria described in section 3.1. The colour coding indicates orbits that pass through strong tidal fields (red), as well as those that are less disruptive (blue). The variation of R_G of the clusters marked a, b, c and d are shown in Fig. 3.

4.2 Disruption time for each orbit as a function of Galactic environment

To assess the role that the Galactic environment (i.e., the type of orbit) played in the evolution of NGC 6791, we model the cluster as described above and place it on each one of the orbits that meet the criteria described in Section 3.1. The orbits found in our orbital analysis start in the inner disc, $3 < R/\text{kpc} < 5$, a region of strong tidal fields, which will cause significant mass loss of the cluster. The mass loss due to tidal interactions depends on how long the orbit stays in the inner disc.

Figure 2 shows the evolution of the cluster’s mass with time, for the migrating orbits from model B. All clusters are initialized with the same properties (30,000 stars, each of $1 M_\odot$; as well as an initial r_h of 6 pc), the only difference between the models is the orbit.

From Figure 2 we see that the evolutionary paths are diverse, all orbits end up at the solar circle, $R_{GC} \approx 8 \text{ kpc}$, but before reaching that distance some of them spend more time in the inner disc. Moreover, some orbits approach the Galactic centre (closer than their starting positions) before they are displaced to larger radii. This type of orbits take the cluster to Galactic environments with strong tidal fields, causing the cluster to rapidly lose mass and to be disrupted in a short time. On the other hand, there also exist orbits that, although starting in the inner disc, are quickly displaced to larger radii, hence a cluster moving on one of those orbits will not interact with strong tides for most of its lifetime.

To better illustrate how the mass loss of the cluster depends on the orbit it follows, we show in Figure 3 the galactocentric radius R_{GC} as a function of time for four different orbits (these orbits are highlighted in Figure 2); the colour code indicates the strength of the tides at every point in the orbit. We choose these four orbits because they exhibit the different behaviours described above. All of them start their evolution in the inner region of the disc, where the tidal field is strong, but the time they spend there varies from one to another. For the orbits in Figure 3 the inhospitability of the

Galactic environment increases from top to bottom. The orbit in the top makes a quick excursion to smaller radii, but then it is displaced to larger radii in less than 1 Gyr, and stays there, where the tidal interaction with the Galaxy is less destructive. The next orbits stay longer periods of time at small radii, increasing the interaction of the cluster with strong tides, and hence increasing the mass loss. Notice that the most violent orbits stay close to the Galactic centre for 3 or even 5 Gyr before they are displaced to regions of less destructive tides. Hence, the different behaviour of each orbit determines the mass loss and evolution of the cluster, as shown in Figure 2.

As a consequence of the mass loss dependence on the type of orbit, and to assure that our models end up with the correct mass after an 8 Gyr evolution, we need to initialize the simulated clusters with different initial masses. For the next set of simulations all clusters are initialized with a $r_h = 6 \text{ pc}$, and we impose the condition that at $t = 8 \text{ Gyr}$ the remaining mass should be within the range $4 \times 10^3 < M/M_\odot < 6 \times 10^3$; the first simulation starts with an initial mass, $M_0 = 3 \times 10^4 M_\odot$; if after 8 Gyr the remaining mass is not within those values, then the simulation is repeated with increasing or decreasing M_0 . By performing this iteration, we can assign the optimal initial mass for the cluster according to the type of orbit and Galactic environment.

Figure 4 shows the initial mass exploration, and we can see that, unlike what happens in Figure 2, all clusters survive and are still massive at $t = 8 \text{ Gyr}$. Notice that it is possible to get all our models to converge to similar evolutionary stages ($M \approx 5 \times 10^3 M_\odot$) as long as we adopt a wide range of initial masses. As expected, clusters moving on more destructive orbits, i.e., interacting with strong tides, will need to be massive at their formation ($M > 5 \times 10^4 M_\odot$). On the other hand, putting the cluster on a less violent orbit allows to adopt an initial mass significantly smaller compared to the one needed for the more violent orbits ($M > 1.8 \times 10^4 M_\odot$).

Figures 2-4 illustrate the importance of the Galactic environment in determining the possible initial mass of NGC 6791. This implies that, unless we know the exact orbit, this cannot be uniquely determined.

4.3 The effect on survivability of initial mass and of initial half-mass radius

From Figures 2 and 4 we notice that to assure the survival of the cluster, it must have been born significantly more massive than it is at the present time. Actually, its survivability also depends on the initial concentration in the distribution of stars (i.e., the half mass radius of the system at birth). A high concentration of stars will require a relatively small initial mass, while a sparse system will require a greater initial mass in order to assure that the cluster will not be totally disrupted after an 8 Gyr evolution.

By modeling NGC 6791, as described in Section 4.1, we explore here a possible correlation between M_0 and the initial r_h of the cluster. We study all the possible combinations of (M_0, r_h) within the intervals $6 \times 10^3 < M_0/M_\odot < 1.5 \times 10^5$ and $3 < r_h/\text{pc} < 13.5$, these intervals are explored with increments $\Delta M_0 = 10^3 M_\odot$ and $\Delta r_h = 0.5 \text{ pc}$. From this set of simulations, we choose the ones where the mass of the cluster, after an 8 Gyr evolution, is within $2 \times 10^3 < M/M_\odot <$

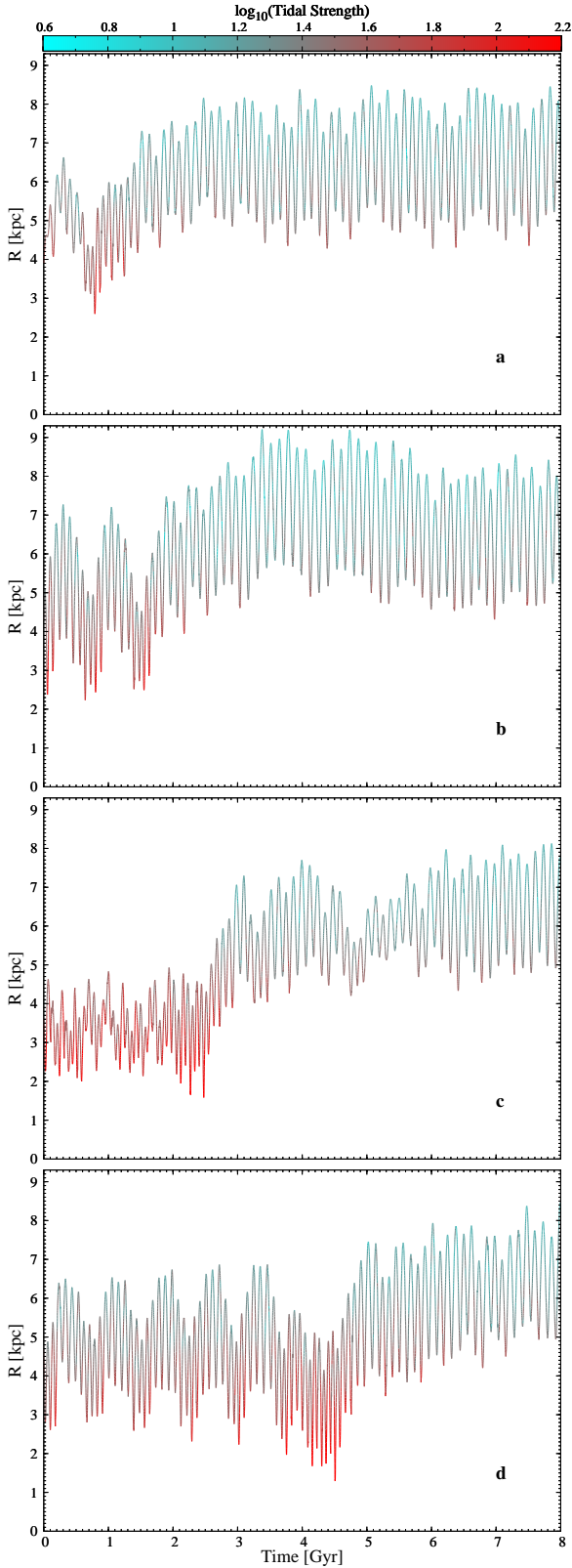


Figure 3. Evolution of the cluster’s galactocentric radius R_{GC} for four different orbits that start between 3 and 5 kpc. The colour coding indicates the strength of the tides at each point on the orbit. Because the initial conditions of the clusters are the same, this plot illustrates the importance of the orbital evolution.

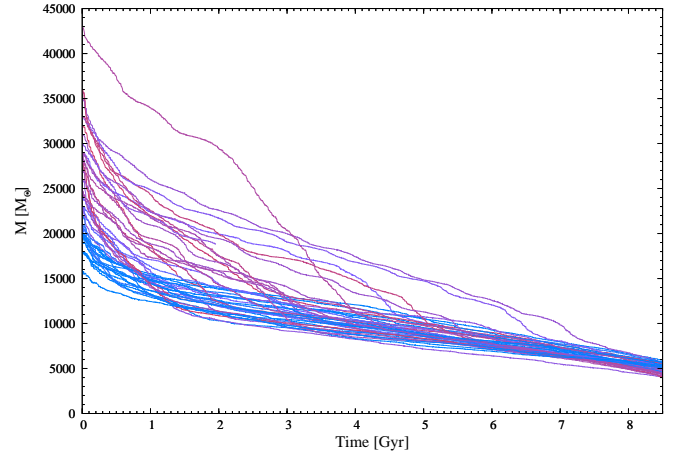


Figure 4. Mass evolution for the stellar cluster evolved along the orbits integrated with the Galactic model B, and that meet the criteria described in section 3.1. The colour coding indicates orbits that pass through strong tidal fields (red), as well as those that are less disruptive (blue).

8×10^3 . Here we use the same orbit for all modeled clusters in order to isolate the role of M_0 and r_h in the evolution of the cluster.

The resulting relation from this exploration of values for M_0 and r_h is shown in Figure 5. The dispersion of values is small, showing a clear correlation between initial mass and initial half mass radius, which means that these two important properties of the cluster are not independent. For $\log(r_h/\text{pc}) \gtrsim 0.8$ the models follow a line of constant initial half-mass density (i.e. $M \propto r_h^3$). This can be understood as follows: these models dissolve under the influence of tidal perturbations (i.e. relaxation and stellar evolution are not included), which occurs on a time-scale that is proportional to the cluster density (e.g. Spitzer 1958 and section 6). Because we forced all clusters to survive, all surviving initial conditions have the same initial density.

These models do not include the effect of stellar evolution and two-body relaxation, which both tend to expand the cluster and will therefore speed up the mass-loss. The initial mass of the models in Fig. 4 are therefore lower limits. In the next section we consider all effects combined with an N -body model.

5 N -BODY MODELS OF NGC 6791

In addition to the properties previously mentioned, Dalessandro et al. (2015) find evidence of tidal distortions in the outer parts, and provide a King model fit for the inner part of the cluster. Meanwhile, King et al. (2005) present an estimate of the cluster’s mass function (MF) (defined as the number of stars in linear mass bins $N(m)dm$), which is rather flat implying that the cluster has lost a large number of its low-mass stars (assuming a universal IMF).

A comparison with these observables gives us the opportunity to better constrain our models and find the more likely properties of NGC 6791 at its moment of birth. To perform this, a more detailed modeling of the cluster needs to be done. For this part of the work we employ NBODY6TT

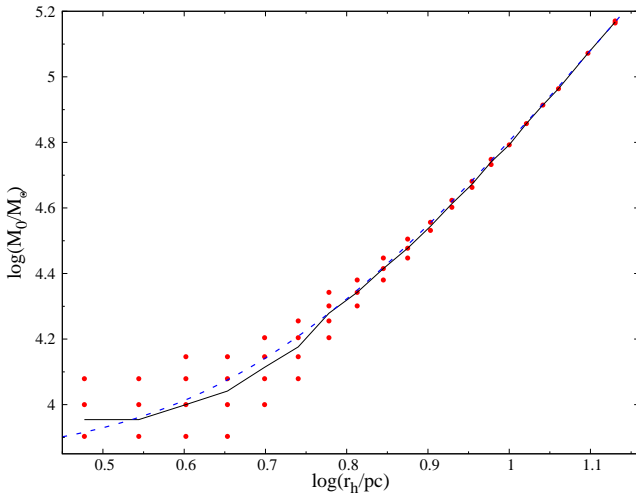


Figure 5. Relation between initial mass M_0 and initial half mass radius r_h (black solid line). Every point corresponds to models that after an 8 Gyr evolution still have a remaining mass similar to the one of NGC 6791. The data can be adjusted by a cubic relation between M_0 and r_h , indicated here with dashed blue line.

a state-of-the-art direct N -body code, a modified version of the direct N -body integrator NBODY6 (Aarseth 2003) optimised for use with Graphics Processing Units (GPUs) (Nitadori & Aarseth 2012), which was specifically designed for modelling collisional star clusters. It solves pairwise gravitational interactions between stars in the cluster and includes synthetic stellar evolution (Hurley et al. 2000, 2002). We here use NBODY6TT ‘Mode A’ to include the tidal field, which relies on user defined tidal tensors which are read in and from which the tidal forces are applied in the tidal approximation (Renaud, Gieles, & Boily 2011).

As shown in previous sections, the initial mass of the cluster was possibly considerably larger than it is now, however the method employed in Section 4.1 does not consider internal evolution, which is an important factor in the cluster’s mass loss process. Because of that, for the N -body modeling of NGC 6791, we initialize the cluster with a mass greater than the one used in Section 4.2. We find the initial mass iteratively. We adopt a Kroupa initial mass function (IMF) (i.e. double power-law with logarithmic slope of -1.3 below $0.5 M_\odot$ and -2.3 above it), with star masses between $0.1 M_\odot$ and $100 M_\odot$, and a r_h of 2.3 pc. Table 3 shows the initial set-up of the cluster, meanwhile the tidal tensor is pre-computed along one of the orbits from Section 3, it is passed to NBODY6TT as described in Renaud, Gieles, & Boily (2011). During the simulation, escapers that reach a distance of two times the tidal radius, r_{tide} , are removed, with $r_{\text{tide}} = 10r_h$.

5.1 Cluster evolution: mass and density

The result of the N -body modeling of NGC 6791, moving on top of one of the less violent migrating orbits, is shown in Figure 6. The cluster loses mass along the entire orbit, with significant stripping at the beginning of its evolution and at the closest approaches to the Galactic centre, as indicated in the bottom panel of Figure 6. A comparison between both

Table 3. Setup for the N -body model of NGC 6791

Initial values of the N -body models.	
Initial mass, M_0	$5 \times 10^4 M_\odot$
Number of stars	8×10^4
Initial Mass Function	Kroupa
Maximum star mass	$100 M_\odot$
Minimum star mass	$0.1 M_\odot$
Average star mass	$0.637 M_\odot$
Half-mass radius	2.3 pc

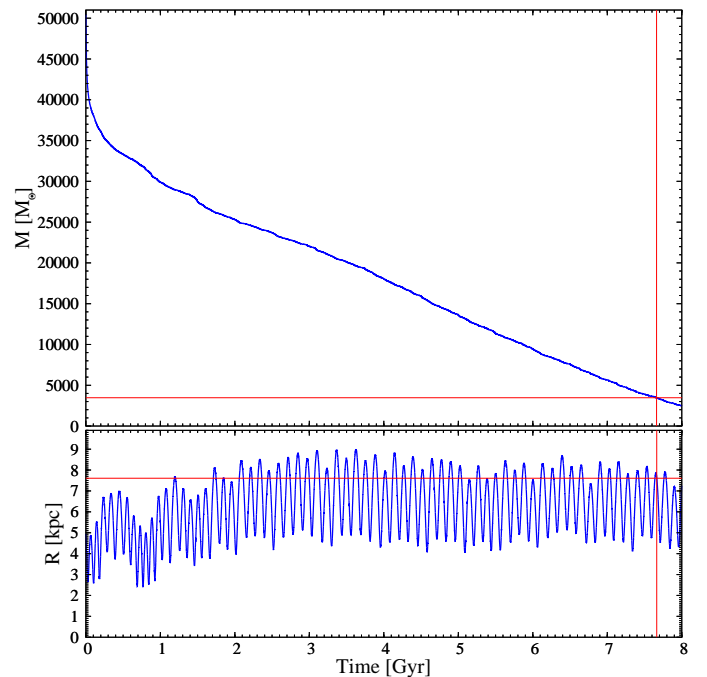


Figure 6. Top: cluster stellar mass as a function of time. Bottom: evolution of the Galactocentric radius R_{GC} for the orbit of the cluster. Red lines indicate the position and mass of the cluster at the moment its galactocentric distance, PM, and radial velocity, are similar to the current ones of NGC 6791.

panels shows that the slope of the mass curve is clearly modified every time the cluster enters a region of strong tides, this means that the orbit of the cluster is imprinted in its evolution, and determines its final stage.

As described in section 3.1, this particular orbit meets our selection criteria at 7.66 Gyr, at that moment in the simulation the cluster is quite massive, $M = 3473 M_\odot$, as indicated in the top panel of Figure 6. By setting the cluster to follow one of the less violent migrating orbits that ends up to be similar to the current one for NGC 6791, but also fulfilling the condition of ending with a massive cluster after the entire evolution, the selected initial mass for this model, $M_0 = 5 \times 10^4 M_\odot$, give us a lower limit for the predicted mass of NGC 6791 at its moment of birth.

Figure 7 shows the evolution of r_h and core radius, r_c . The cluster undergoes an expansion period of ~ 3 Gyr before reaching approximately 50% of its initial mass, then it undergoes core-collapse. After ~ 5 Gyr, and until 7.6 Gyr, r_h changes rather slowly until its final value. Despite the time-

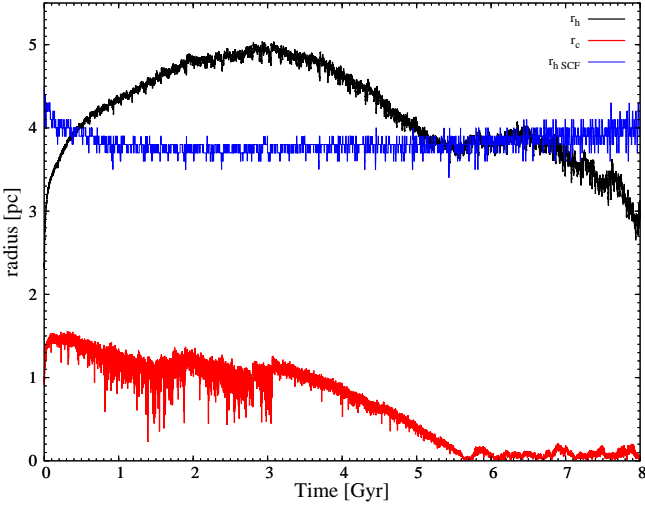


Figure 7. Evolution of the half mass radius r_h (black) and core radius r_c (red) for the simulation shown in Figure 6. For comparison, we also indicate the r_h for a model described with the SCF method (blue).

dependent tidal field, the general behaviour of $r_h(t)$ (i.e. expansion followed by contraction) is similar to the evolution of clusters in static tides (Gieles, Heggie, & Zhao 2011). For comparison, Figure 7 also shows the evolution of r_h for a cluster modeled with the method described in Section 4.1. Note that because two-body relaxation is not considered, the cluster does not undergo the expansion nor the collapse seen in the N -body model. Because of the lack of significant expansion, for a cluster modelled with the SCF technique, the mass loss can be underestimated; this becomes noticeable in high concentrated models, where the evolution would differ from that of the N -body model shown in Figure 6.

Another known property for NGC 6791 is its projected density. Dalessandro et al. (2015) determine the projected density profile using direct counts of stars along the main sequence in the magnitude range $18 < g' < 21.5$. In order to compare with the data, from the simulation we select stars within the same magnitude range, which is translated to the mass range $0.73 < m/M_\odot < 1.08$. For stars with those masses, Figure 8 shows the projected number density profile of the N -body model at 7.6 Gyr, as well as the data from Dalessandro et al. (2015). The (post-collapse) N -body model is more centrally concentrated than NGC 6791. The number density profile suggests that NGC 6791 has not yet reached core collapse. The reason that our N -body model has already experienced core collapse could be due to several reasons: (1) we did not include primordial binary stars, which delay core collapse (e.g. Giersz & Heggie 2011); (2) the stellar-mass black holes received the same super nova kick as the neutron stars such that few black holes are retained; a black hole population could also inflate the (visible) core (e.g. Merritt et al. 2004; Mackey et al. 2008; Peuten et al. 2016). The N -body model reproduces the ‘kink’ in the number density profile near $R \sim 800''$, which is due to so-called potential escapers, which are energetically unbound stars that are associated with the cluster because of their long escape time (Fukushige & Heggie 2000)

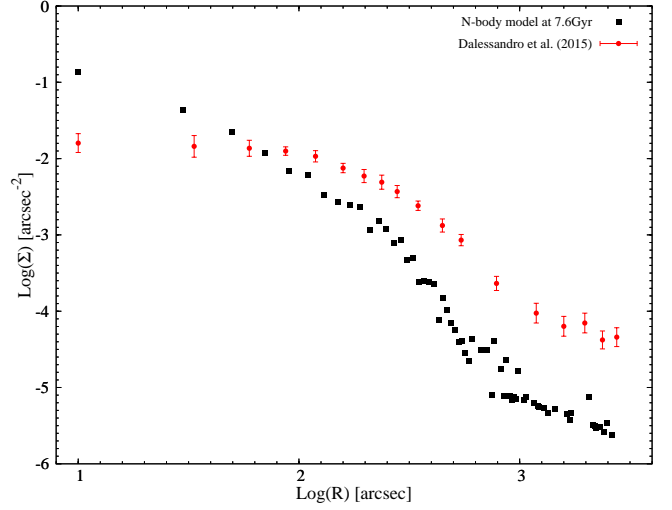


Figure 8. Number density profile in projection for the N -body model at 7.6 Gyr as a function of projected radius (black squares), compared to the observed number density profile from Dalessandro et al. (2015).

and are found predominantly in the outskirts of star clusters (Küpper et al. 2010; Claydon et al. 2017). Just as tidal streams, the potential escapers are more visible in clusters that are near dissolution (in terms of remaining mass fraction, Balbinot & Gieles 2017), as is the case for NGC 6791.

5.2 Stellar mass function

The observed mass function (MF) of a star cluster gives insights into its IMF and its dynamical evolution. There is an observed correlation between the MF and the galactocentric distance, being steeper for clusters more distant from the galactic centre (Djorgovski et al. 1993); a correlation also found in N -body simulations (Vesperini & Heggie 1997; Baumgardt & Makino 2003). Several studies have shown that for a given IMF, the slope of the present-day MF is a good proxy of the fraction of the initial cluster mass that still remains in the cluster (e.g. Baumgardt & Makino 2003; Trenti et al. 2010). This means that we can use the shape of the MF and the present-day mass to estimate the initial mass of NGC 6791, which we can compare to what we find in the N -body model.

Using the Hubble Space Telescope (HST), King et al. (2005) derive the present-day MF for NGC 6791. They found that the MF is fairly flat between $0.1 M_\odot$ and $1 M_\odot$. We follow the MF with time in the simulation and compare the result to the observations of King et al.

In order to make a proper comparison with the observed MF, notice that the HST data of King et al. (2005) is not covering the entire cluster. Those observations were made with the Wide Field Channel (WFC) of the Advance Camera for Surveys (ACS), within a field centred $1.5'$ away from the cluster centre, and the field of view of the WFC is $3.3' \times 3.3'$. This means that the camera covered distances up to $3.15'$ from the cluster centre. On the other hand, from the King model fit of Dalessandro et al. (2015), we estimate a $3D r_h \approx 5'$, which means that the MF derived from the HST

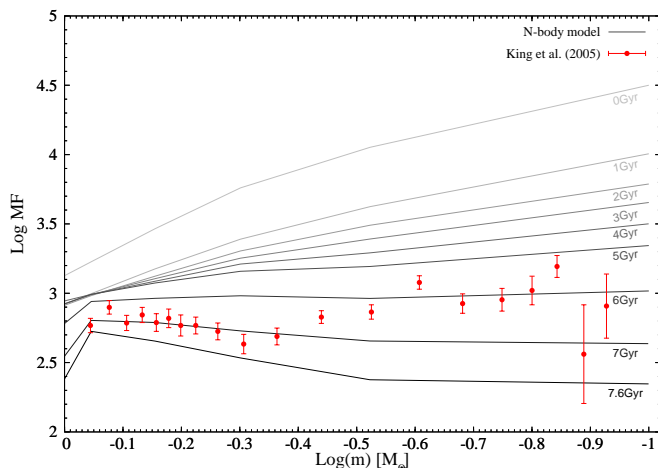


Figure 9. Stellar MF for different ages of the cluster.

data is biased towards the centre of the cluster. To compare with the MF reported by King et al. (2005) we select stars in the simulation within distances less than $3.15'$, which for an adopted distance to the cluster of 4.01 kpc (Table 2) translates into a MF for stars within a radius of $r = 3.66$ pc.

Figure 9 shows the MF, for different ages of the cluster. The MF flattens as the cluster evolves; this happens as a consequence of the mass loss via the preferential escape of low-mass stars, which is greater in the first few Gyr, as shown in Figure 1. Notice that the MF from the data is fairly flat (the slope of the MF is significantly smaller than the one of the assumed IMF), meanwhile the MF from the model reaches a similar slope at around ~ 7 Gyr, consistent with the age of NGC 6791.

A star cluster loses mass through the tidal boundary due to two-body relaxation and tidal interaction with the Galaxy; both processes flatten the global MF (Vesperini & Heggie 1997; Baumgardt & Makino 2003). The strength of the tides experienced by the cluster, and hence the mass loss due to this mechanism, will be larger in the inner regions of the Galaxy.

With a large set of N -body models of multimass clusters evolving in a Galactic tidal field, Baumgardt & Makino (2003) found a dependence of the slope of the MF on the mass fraction lost from a cluster. They parameterize the mean evolution of the slope by

$$\alpha = \alpha_0 - \exp \left[0.67 - 6.19 \frac{M}{M_0} - 3.24 \left(\frac{M}{M_0} \right)^2 \right], \quad (1)$$

where M is the remaining mass of the cluster, M_0 its initial mass, α is the power-law slope of the MF at any point in the evolution of the cluster, while α_0 is the slope of the IMF. This parameterization allows to infer the initial mass of NGC 6791 from its present-day MF and mass.

Assuming a Kroupa IMF, $\alpha_0 = 1.3$ in the mass range $0.1 < m/M_\odot < 0.5$, while a linear fit to the data from King et al. (2005) returns the present-day slope $\alpha = 0.2$. By taking this values as input for equation (1) we infer a current mass to initial mass ratio of $M/M_0 \approx 0.089$; and with the current mass of NGC 6791, $M \sim 5000 M_\odot$ (Platais et al.

2011), we infer an initial mass of $M_0 = 56180 M_\odot$. This estimation is in good agreement with our predicted value of $M_0 = 5 \times 10^4 M_\odot$ from the N -body model placed on top of a migrating orbit.

Figure 9 also shows that a flatter IMF and less mass loss would give a similar present-day MF. However, for an assumed IMF, the present-day MF tells us directly how much mass the cluster has lost; but the amount of mass lost can also be estimated by assuming a dynamical history. Because we found agreement between these two mass loss estimations, we conclude that the combination of the assumed IMF and the dynamical history is correct. In this sense we corroborate that, because the slope of the data by King et al. (2005) is significantly smaller than the slope of the plausible adopted IMF, the observed MF of NGC 6791 is fairly flat.

Finally, for comparison, we can estimate the slope of the present-day MF of a cluster that was born and has always been orbiting at 8 kpc from the galactic centre. Again here we use the expressions by Baumgardt & Makino (2003): first for the lifetime of a cluster moving in a external potential

$$\frac{T_{\text{diss}}}{\text{Myr}} = 1.91 \left[\frac{N}{\ln(0.02N)} \right]^{0.75} \frac{R_G}{\text{kpc}} \left(\frac{V_G}{220 \text{ km s}^{-1}} \right)^{-1} (1 - \epsilon), \quad (2)$$

where T_{diss} is the lifetime of the cluster, N is the number of cluster stars, R_G the galactocentric distance, V_G the circular velocity of the galactic model, and ϵ the eccentricity of the orbit. Then we use the parameterization for the evolution of the MF slope as a function of the time elapsed until cluster dissolution

$$\alpha = \alpha_0 - 1.51 \left(\frac{T}{T_{\text{diss}}} \right)^2 + 1.69 \left(\frac{T}{T_{\text{diss}}} \right)^3 - 1.5 \left(\frac{T}{T_{\text{diss}}} \right)^4. \quad (3)$$

Under the assumption that the cluster has moved in circular orbit, at the solar circle $R_G = 8$ kpc, for 8 Gyr, equation (2) gives a dissolution time of $T_{\text{diss}} \approx 12$ Gyr; taking this value as input for equation (3), the predicted slope of the present-day MF at the low-mass end is $\alpha \approx 0.83$, which corresponds to a MF significantly steeper than the observed one ($\alpha \approx 0.2$).

In this way the result from the parameterization of the MF slope (Baumgardt & Makino 2003) applied to the observational data of King et al. (2005) is a validation of the initial mass we infer for NGC 6791. Also, showing that the observed MF is flatter than what is expected for a cluster that has always been at 8 kpc supports our hypothesis that NGC 6791 experienced stronger tides in the past.

5.3 Velocity dispersion

Regarding the velocity dispersion, Carraro et al. (2006) obtain radial velocities for a subsample of 15 giant stars in NGC 6791 and report a radial velocity dispersion of $\sigma_r = 2.2 \pm 0.4 \text{ km s}^{-1}$. More recently, Platais et al. (2011) note that if a King model is assumed to describe the inner mass profile of NGC 6791, then the projected velocity dispersion averaged within r_h should be $\sigma_r \simeq 0.75 \text{ km s}^{-1}$, a value significantly lower than the one reported by Carraro et al. (2006).

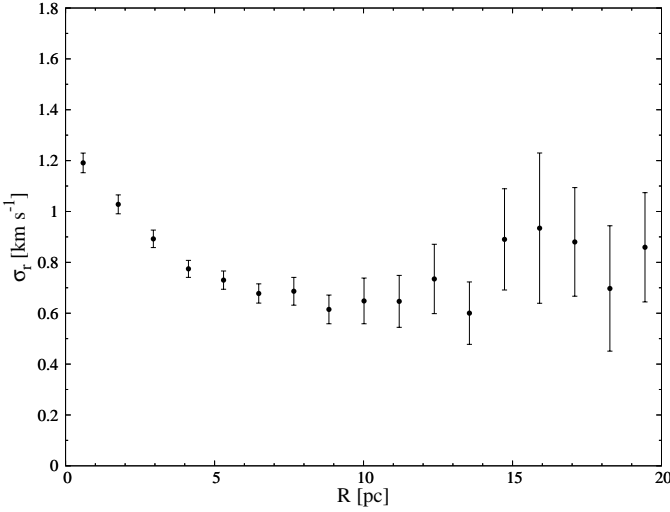


Figure 10. Projected velocity dispersion as a function of projected radius within the cluster.

In Figure 10 we compute the projected velocity dispersion as a function of radius within the cluster, for the model at 7.6 Gyr. Notice that the dispersion in projected velocities is small near the cluster centre, and increases at the boundaries, with a peak value near the tidal radius. Hence, in our models we found that σ_r inside the half mass radius is small, similar to the expected value from Platais et al. (2011), and much lower than the one reported by Carraro et al. (2006). The high dispersion measured by Carraro et al. may be due to orbital motions of binary stars that increase the velocity dispersion, and which are not included in our N -body model, nor in the (virial) estimate of Platais et al.

From Figure 10 we can see two different behaviours; in the central parts of the cluster σ_r systematically decreases with radius, however, for larger radii, it remains constant or even increases. This increase is most likely due to the aforementioned potential escapers (Fukushige & Heggie 2000; Claydon et al. 2017).

6 THE DISRUPTIVE EFFECT OF INTERACTIONS WITH GIANT MOLECULAR CLOUDS

In our N -body model we did not include molecular gas, and it is well-known that interactions with giant molecular clouds (GMCs) are an efficient cluster disruption mechanism (Spitzer 1958; Gieles et al. 2006). Here we quantify the disruptive effect of the Milky Way disc by using a simple model for the gas distribution in the Milky Way and by following one of our cluster orbits through the gas.

Spitzer (1958) showed that the disruption timescale as the result of impulsive tidal shocks from passing GMCs can be expressed as

$$\tau_{\text{GMC}} = \gamma_{\text{GMC}} \rho_{\text{h}}, \quad (4)$$

where ρ_{h} is the average density within the half-mass radius of the cluster, and γ_{GMC} depends on the properties of the molecular gas as

$$\gamma_{\text{GMC}} \propto \frac{\sigma_{\text{rel}}}{\Sigma_{\text{GMC}} \rho_{\text{gas}}}, \quad (5)$$

with σ_{rel} is the dispersion of the relative velocities between the cluster and the GMCs, Σ_{GMC} is the surface density of individual GMCs and ρ_{gas} is the volume density of cold molecular gas.

We consider a density profile for the cold molecular gas of the form

$$\rho_{\text{gas}}(R_{\text{GC}}, z) = \rho_0 \exp\left(-\frac{R_{\text{GC}}}{L}\right) \text{sech}^2\left(-\frac{Z}{2h}\right). \quad (6)$$

Here $R_{\text{GC}} = \sqrt{X^2 + Y^2}$ is the distance to the Galactic centre when in the midplane and Z is the height above the disc. The (vertical) velocity dispersion is $\sigma_z(R_{\text{GC}}) = h\sqrt{8\pi G\rho_0 \exp(-R_{\text{GC}}/L)}$ and is independent of Z . We use a scale length of $L = 2.5$ kpc and a scale height of $h = 60$ pc (Binney & Tremaine 2008) and we chose $\rho_0 = 0.74 M_{\odot}/\text{pc}^3$, such that the mid-plane density at the solar radius ($R = 8$ kpc) equals $0.03 M_{\odot}/\text{pc}^3$ (Solomon et al. 1987).

We follow a particle orbit through this disc and determine the quantity

$$f = \left(\frac{\int_0^{8 \text{ Gyr}} \gamma_{\text{GMC}}^{\odot} / \gamma_{\text{GMC}}(t') dt'}{8 \text{ Gyr}} \right)^{-1} \quad (7)$$

where $\gamma_{\text{GMC}}^{\odot}$ is the quantity in equation (4) for the disruption in the mid-plane in the solar neighbourhood. For the orbit described in section 5.1 we find $f \simeq 2.3$. Gieles & Renaud (2016) showed that because of the self-limiting nature of tidal shocks, the timescale for dissolution scales as $\gamma_{\text{GMC}}^{1/3}$. Taking the harmonic time average of this quantity, we find $f \simeq 1.9$.

From this exercise we find that, despite the fact that NGC 6791 formed near the Galactic centre, the average effect of disruption by GMCs during its life is less important than in the mid-plane at the solar radius. This can be understood by the large vertical excursions from the disc, where the GMC density is low.

Using the results of Gieles & Renaud (2016), we estimate that the (average) disruption time-scale by GMCs is ~ 6 Gyr such that the initial mass of NGC 6791 could have been a factor of ~ 2 higher than what we derived in Section 5 if we had included interactions with the molecular gas. The initial mass could not have been much higher, otherwise the MF would have been even flatter.

7 DISCUSSION

7.1 Plausibility of radial migration

Several papers have studied the orbit of NGC 6791, trying to test the plausibility of a radial migration scenario that displaced the orbit of the cluster from the inner Galaxy to its present-day location (Carraro et al. 2006; Bedin et al. 2006; Wu et al. 2009; Jilková et al. 2012). Most of these works integrate orbits within galactic potentials that are either axisymmetric or incorporate bar and spiral arms in a rather

simplified way (a potential that does not try to reproduce an existing mass distribution). It is known that in order for radial migration to happen, the orbit should modify its angular momentum, a process not possible within an axisymmetric potential. In this respect, by including a bar and spiral arms, [Jílková et al. \(2012\)](#) present an improvement over previous works, however they still treat the spiral arms as a perturbation not based in physical overdensities, which underestimates their dynamical effect ([Pichardo et al. 2003](#)); in addition to this; the authors are missing an extra velocity transformation that is key for their study, so we should caution making conclusions about the orbit of NGC 6791 based on their analyses.

Although some authors argue that the radial migration process is not efficient enough to move the cluster more than a couple of kpc, nor able to lift it to its present position ([Jílková et al. 2012](#); [Linden et al. 2017](#)), in this work, employing a Galactic model based on physical mass distributions of a bar and detailed spiral arms, we find that a fraction of the newly formed clusters will eventually (8 Gyr) migrate more than 4 kpc and be lifted more than 800 pc away from the disc mid-plane; specifically, we found abundant examples of orbits that match the current PMs and high altitudes of NGC 6791 that started their evolution in the inner thin disc.

Due to the dynamical chaotic nature of the system (produced by the interactions with the bar and the spiral arms) we find hundreds of distinct orbits that fulfill our selection criteria (i.e. orbits whose present day orbital parameters correspond to those observed in NGC 6791); such orbits have very different initial conditions and very different overall trajectories, and it is therefore not possible to define an exact initial position, nor the amount of encounters experienced during the orbit.

7.2 Evidence supporting the formation in the inner Galaxy

The evidence that links the formation place of NGC 6791 to the inner Galaxy comes from different observables: It is one of the most metal-rich open clusters in the Galaxy, $[\text{Fe}/\text{H}] \sim +0.40$. Stars with the age of NGC 6791 and with similar $[\text{Fe}/\text{H}]$ are not present at the galactocentric distance of the cluster, but are found in the inner thin disc and in the bulge, $3 \text{ kpc} < R_0/\text{kpc} < 5$. More recently, [Linden et al. \(2017\)](#), using the APOGEE DR13 dataset, placed NGC 6791 in the $[\alpha/\text{Fe}]$ vs. $[\text{Fe}/\text{H}]$ plane; the cluster's position on this plane strongly suggests a connection with the MW bulge as well as with the inner thin disc. However, Linden et al. dismiss an origin in the thin disc arguing that it is unlikely for a radial migration mechanism to operate by several kpc, and especially to account for the current cluster's high altitude above the plane. Although such arguments could prove that it is unlikely that any single cluster would migrate and raise so much, when there are thousands of clusters that are born, it becomes a fact that a few of them will migrate and raise just as much, here we found that the mechanism exists and can reproduce the current orbit of NGC 6791.

On the other hand, HST observations reveal a rather flat stellar mass function in the central regions of NGC 6791 ([King et al. 2005](#)). It is expected that the MF in a stellar cluster flattens with time due to the steady tidal stripping

of mainly the low mass stars. However, the mass loss of the cluster, by removing these stars, must be very efficient in order to achieve a totally flat MF.

Regarding the mass loss, [Dalessandro et al. \(2015\)](#) find signatures of tidal distortions in the density distribution of NGC 6791, suggesting that the cluster is still experiencing mass loss. Based on this evidence, the authors argue that, at some point during its evolution, NGC 6791 may have lost an important fraction of its original mass.

Notice that the observed tidal distortions and flat MF require a significant mass loss to be explained, further supporting the scenario in which NGC 6791 was formed in the inner thin disc or in the bulge (where the tidal field is strong), and undermining the suggestion that it was formed in the nearby thick disc (where the tidal field is much weaker). However, these two observed properties are not enough to restrict the formation place of NGC 6791 because a significant mass loss can also be achieved during violent encounters of the cluster with different Galactic structures at any point along its orbit.

Nonetheless, the high metallicity of NGC 6791 is a key property and the clearest clue about its origin. Its value, along with its age, places the cluster's birth at the inner thin disc or in the bulge, $3 < R_0/\text{kpc} < 5$. In this work we show that it is possible that the cluster migrated from there to its current orbit, and survived.

8 CONCLUSIONS

With the use of an observationally motivated, three dimensional Galactic mass model, we perform a comprehensive orbital study of the enigmatic open cluster NGC 6791. We integrate half million orbits, representing the MW stellar disc, for 8 Gyr to find those with similar position, proper motion, and radial velocity to the current values of NGC 6791.

Contrary to previous results that claim that radial migration is inefficient in moving the cluster to its present position (e.g. [Jílková et al. 2012](#); [Linden et al. 2017](#)), we find 240 examples of orbits that match the current position and velocity of NGC 6791. We expect that out of every 420 massive clusters that were born between 7.5 and 8.5 Gyr ago, with a galactocentric radius between 3 and 5 kpc, one would survive to this day, be far away from the plane, be anomalously metal rich, and be observable from Earth. I.e. there is a probability that an orbit could have suffered an outward radial migration that brought the cluster to its current galactocentric position and its current distance from the plane. This scenario would explain its high metallicity, in spite of its old age.

As a consequence of the previous point, to speak of an exact initial position, or of specific encounters suffered by the orbit of NGC 6791, becomes meaningless in view of its highly chaotic nature produced by the interactions with the bar and the spiral arms.

In order to test the survival of a cluster within the found family of orbits that matches NGC 6791 orbital parameters, we perform two studies, one based on a self-consistent field technique and another based on direct N -body models including the time-dependent Galactic tides and the effects of stellar evolution.

The Galactic environments the cluster went through,

play a key role in its evolution, it determines the possible initial mass of NGC 6791. This implies that, unless we know the exact orbit, the mass cannot be uniquely determined. Nevertheless, in order to endure violent Galactic environments, the cluster should have been born significantly more massive ($\sim 5 \times 10^4 M_{\odot}$) than it is today ($\sim 5 \times 10^3 M_{\odot}$).

As a byproduct of an efficient early tidal stripping, achievable in the strong tidal field of the inner Galaxy, our simulations reproduce a flat stellar mass function, as observed for NGC 6791. Therefore, the birth place and journeys of NGC 6791 are imprinted in its chemical composition, in its mass loss, and in its flat stellar mass function, further confirming its origin in the inner thin disc or in the bulge.

ACKNOWLEDGEMENTS

We thank Lucie Jílková and Giovanni Carraro for discussions on their model and in particular for redoing their orbit calculations with the updated velocities which brought their results in better agreement with our findings (see Section 3). We would like to thank Florent Renaud and Emanuele Dalessandro for fruitful discussions, and an anonymous referee for an insightful review of this work. We are also grateful to Sverre Aarseth and Keigo Nitadori for making NBODY6 publicly available. We acknowledge DGTIC-UNAM for providing HPC resources on the Cluster Supercomputer Miztli. L.A.M.M. and B.P. acknowledge CONACYT Ciencia Básica grant 255167 and DGAPA PAPIIT IG 100115. A.P. acknowledges DGAPA-PAPIIT through grant IN-109716. L.A.M.M. acknowledges support from DGAPA-UNAM postdoctoral fellowship. M.G. acknowledges financial support from the Royal Society (University Research Fellowship) and the European Research Council (ERC StG-335936, CLUSTERS). L.A.M.M. thanks the ERC for partially funding a visit to Surrey where most of this work was done.

REFERENCES

- Allen C., Santillán A., 1991, *Rev. Mex. Astron. Astrofis.*, 22, 255
 Antoja, T., Valenzuela, O., Pichardo, B., et al. 2009, *ApJL*, 700, L78
 Antoja T. et al., 2014, *A&A*, 563, A60
 Aarseth S. J. 2003, *Gravitational N-Body Simulations*, by Sverre J. Aarseth, pp. 430. ISBN 0521432723. Cambridge, UK: Cambridge University Press, November 2003., 430
 Balbinot E., Gieles M., 2017, submitted (arXiv:1702.02543)
 Baumgardt, H., & Makino, J. 2003, *MNRAS*, 340, 227
 Bedin, L. R., Piotto, G., Carraro, G., King, I. R., & Anderson, J. 2006, *A&A*, 460, L27
 Benjamin R. A. et al., 2005, *ApJL*, 630, L149
 Bensby, T., Yee, J. C., Feltzing, S., et al. 2013, *A&A*, 549, A147
 Binney, J., & Tremaine, S. 2008, *Galactic Dynamics*, second edition (Princeton University Press)
 Blum R. D., 1995, *ApJL*, 444, L89
 Brogaard, K., Bruntt, H., Grundahl, F., et al. 2011, *A&A*, 525, A2
 Brogaard, K., VandenBerg, D. A., Bruntt, H., et al. 2012, *A&A*, 543, A106
 Carraro, G., Villanova, S., Demarque, P., et al. 2006, *ApJ*, 643, 1151
 Churchwell, E., Babler, B. L., Meade, M. R., et al. 2009, *PASP*, 121, 213
 Claydon, I., Gieles, M., & Zocchi, A. 2017, *MNRAS*, 466, 3937
 Clutton-Brock, M. 1972, *Ap&SS*, 16, 101
 Clutton-Brock, M. 1973, *Ap&SS*, 23, 55
 Cunha, K., Smith, V. V., Johnson, J. A., et al. 2015, *ApJL*, 798, L41
 Cox, D. P., & Gómez, G. C. 2002, *ApJS*, 142, 261
 Dalessandro, E., Miocchi, P., Carraro, G., Jílková, L., & Moitinho, A. 2015, *MNRAS*, 449, 1811
 Davies, B., de La Fuente, D., Najarro, F., et al. 2012, *MNRAS*, 419, 1860
 de la Fuente Marcos, R., & de la Fuente Marcos, C. 2008, *ApJL*, 685, L125
 Dias, W. S., Alessi, B. S., Moitinho, A., & Lépine, J. R. D. 2002, *A&A*, 389, 871
 Djorgovski, S., Piotto, G., & Capaccioli, M. 1993, *AJ*, 105, 2148
 Drimmel, R., & Spergel, D. N. 2001, *ApJ*, 556, 181
 Dwek E. et al., 1995, *ApJ*, 445, 716
 Figer, D. F., Najarro, F., Gilmore, D., et al. 2002, *ApJ*, 581, 258
 Freeman, K. C. 1970, *ApJ*, 160, 811
 Freudenreich H. T., 1998, *ApJ*, 492, 495
 Friel, E. D. 1995, *ARA&A*, 33, 381
 Fukushige, T., & Heggie, D. C. 2000, *MNRAS*, 318, 753
 García-Berro, E., Torres, S., Althaus, L. G., et al. 2010, *Nature*, 465, 194
 Gerhard O., 2011, *MSAIS*, Vol. 18, 185
 Gieles, M., Portegies Zwart, S. F., Baumgardt, H., et al. 2006, *MNRAS*, 371, 793
 Gieles M., Athanassoula E., Portegies Zwart S. F., 2007, *MNRAS*, 376, 809
 Gieles M., Heggie D. C., Zhao H., 2011, *MNRAS*, 413, 2509
 Gieles, M., & Renaud, F. 2016, *MNRAS*, 463, L103
 Giersz M., Heggie D. C., 2011, *MNRAS*, 410, 2698
 Gozha, M. L., Koval', V. V., & Marsakov, V. A. 2012, *Astronomy Letters*, 38, 519
 Gratton, R., Bragaglia, A., Carretta, E., & Tosi, M. 2006, *ApJ*, 642, 462
 Grundahl, F., Clausen, J. V., Hardis, S., & Frandsen, S. 2008, *A&A*, 492, 171
 Hernquist, L., & Ostriker, J. P. 1992, *ApJ*, 386, 375
 Hurley, J. R., Pols, O. R., & Tout, C. A. 2000, *MNRAS*, 315, 543
 Hurley, J. R., Tout, C. A., & Pols, O. R. 2002, *MNRAS*, 329, 897
 Jílková, L., Carraro, G., Jungwiert, B., & Minchev, I. 2012, *A&A*, 541, A64
 Johnson, D. R. H., & Soderblom, D. R. 1987, *AJ*, 93, 864
 Kaluzny, J., & Udalski, A. 1992, *Acta Astron.*, 42, 29
 Kent S. M., 1992, *ApJ*, 387, 181
 King, I. R., Bedin, L. R., Piotto, G., Cassisi, S., & Anderson, J. 2005, *AJ*, 130, 626
 Kinman, T. D. 1965, *ApJ*, 142, 655
 Krabbe, A., Genzel, R., Eckart, A., et al. 1995, *ApJL*, 447, L95
 Küpper, A. H. W., Kroupa, P., Baumgardt, H., & Heggie, D. C. 2010, *MNRAS*, 407, 2241
 Lada, C. J., & Lada, E. A. 2003, *ARA&A*, 41, 57
 Lamers, H. J. G. L. M., Gieles, M., Bastian, N., et al. 2005, *A&A*, 441, 117
 Linden, S. T., Pryal, M., Hayes, C. R., et al. 2017, *ApJ*, 842, 49
 Mackey A. D., Wilkinson M. I., Davies M. B., Gilmore G. F., 2008, *MNRAS*, 386, 65
 Mateo, M. L. 1998, *ARA&A*, 36, 435
 Martínez-Medina, L. A., Pichardo, B., Pérez-Villegas, A., & Moreno, E. 2015, *ApJ*, 802, 109
 Martínez-Medina, L. A., Pichardo, B., Moreno, E., & Peimbert, A. 2016, *MNRAS*, 463, 459
 Martínez-Medina, L. A., Pichardo, B., Peimbert, A., & Moreno, E. 2017, *ApJ*, 834, 58
 Martínez-Medina, L. A., Pichardo, B., Peimbert, A., & Carigi, L. 2017, *MNRAS*, 468, 3615

- Martos, M., Hernandez, X., Yáñez, M., Moreno, E., & Pichardo, B. 2004, MNRAS, 350, L47
- Merritt D., Piatek S., Portegies Zwart S., Hemsendorf M., 2004, ApJ, 608, L25
- Miyamoto, M., & Nagai, R. 1975, PASJ, 27, 533
- Monari, G., Famaey, B., Siebert, A., et al. 2016, MNRAS, 461, 3835
- Moreno, E., Pichardo, B., & Velázquez, H. 2014, ApJ, 793, 110
- Moreno, E., Pichardo, B., & Schuster, W. J. 2015, MNRAS, 451, 705
- Nagata, T., Hyland, A. R., Straw, S. M., Sato, S., & Kawara, K. 1993, ApJ, 406, 501
- Nitadori, K., & Aarseth, S. J. 2012, MNRAS, 424, 545
- Origlia, L., Valenti, E., Rich, R. M., & Ferraro, F. R. 2006, ApJ, 646, 499
- Paumard, T., Genzel, R., Martins, F., et al. 2006, ApJ, 643, 1011
- Pérez-Villegas, A., Gómez, G. C., & Pichardo, B. 2015, MNRAS, 451, 2922
- Peuten M., Zocchi A., Gieles M., Gualandris A., Hénault-Brunet V., 2016, MNRAS, 462, 2333
- Pichardo, B., Martos, M., Moreno, E. & Espresate, J., 2003, ApJ, 582, 230
- Pichardo, B., Martos, M., & Moreno, E. 2004, ApJ, 609, 144
- Pichardo, B., Moreno, E., Allen, C., et al. 2012, AJ, 143, 73
- Piskunov, A. E., Kharchenko, N. V., Röser, S., Schilbach, E., & Scholz, R.-D. 2006, A&A, 445, 545
- Platais, I., Cudworth, K. M., Kozhurina-Platais, V., et al. 2011, ApJL, 733, L1
- Plummer H. C., 1911, MNRAS, 71, 460
- Portail M., Gerhard O., Wegg C., Ness M., 2017, MNRAS, 465, 1621
- Portegies Zwart, S. F., McMillan, S. L. W., & Gieles, M. 2010, ARA&A, 48, 431
- Ramírez Alegría, S., Borissova, J., Chené, A. N., et al. 2014, A&A, 564, L9
- Renaud F., Gieles M., Boily C. M., 2011, MNRAS, 418, 759
- Renaud F., et al., 2015, MNRAS, 454, 3299
- Schönrich, R., Binney, J., & Dehnen, W. 2010, MNRAS, 403, 1829
- Sellwood, J. A., & Binney, J. J. 2002, MNRAS, 336, 785
- Solomon, P. M., Rivolo, A. R., Barrett, J., & Yahil, A. 1987, ApJ, 319, 730
- Spitzer, L., Jr. 1958, ApJ, 127, 17
- Stanek K. Z., Udalski A., Szymański M., KaLuZny J., Kubiak Z. M., Mateo M., Krzemiński W., 1997, ApJ, 477, 163
- Trenti, M., Vesperini, E., & Pasquato, M. 2010, ApJ, 708, 1598
- van der Kruit, P. C. 2002, *The Dynamics, Structure & History of Galaxies: A Workshop in Honour of Professor Ken Freeman*, 273, 7
- Vesperini, E., & Heggie, D. C. 1997, MNRAS, 289, 898
- Weiner B. J., Sellwood J. A., 1999, ApJ, 524, 112
- Wu, Z.-Y., Zhou, X., Ma, J., & Du, C.-H. 2009, MNRAS, 399, 2146
- Zhao H., 1994, PhD thesis, Columbia Univ.